

# Restoration image degraded by a blurred variable in the field

YOUNESS BENTAHAR\*, MOHAMED AFIFI, HANANE DALIMI, SAID AMAR

Laboratory, Engineering and Materials, Physics Department,  
Hassan II University Casablanca, Casablanca, Morocco

\*Corresponding author: bentahar.youness@hotmail.fr

Various methods of deconvolution have been developed for several decades, notably in astronomy and microscopy. The extension of these techniques to the case of a spatially varied blur is currently an open problem. In this work, we consider a zone-invariant point spread function model to take into account blur variation in the image. Thus an algorithm has been used where the minimization of the criterion is performed in parallel on different areas of the image, while taking into account the estimates in the neighboring areas of the sub-images under consideration, so that the final solution is the minimum of the criterion where the blur is spatially varied.

Keywords: blind image deconvolution, restoration, total variation.

## 1. Introduction

The images acquired by the optical imaging systems suffer from degradations due, on the one hand, to the intrinsic properties of the instruments and on the other hand, to the acquisition conditions. Actual optical imaging systems recognized a considerable advance providing high resolution and good contrast photography compared to the first telescopes that were invented in the 15th century. Nevertheless, till now they suffer from some artifacts mainly due to the inherent limitations of the optical instruments as well as the imaging environment. Indeed, optical images are affected by undesired blur which is introduced by different distortion sources. For instance, the diffraction of light through a small circular aperture or imperfect optical lens produces a blur commonly represented by an airy disc [1, 2] which limits the resolution of the acquired image. Astrophysical images, for example, appear blurry because of the turbulence of the atmosphere. In 3D confocal microscopy, the images present essentially a depth defocusing blur and a radial blur associated with the luminous diffraction of the lenses. Moreover, a movement of the lens or objects in the scene during acquisition produces the motion blur. To remedy the effects of blur on the images, many deconvolution techniques have been developed.

For example, in the 3D confocal microscopy, the blur depends on the depth [3–6]. Thus, the blur cannot be considered constant at any point of the image. It is then essential to implement a restoration method in which the function of fuzziness (point spread function – PSF) is spatially variable. This problem has been studied in previous works such as [5, 7–10]. One of the difficulties is the computation time when considering the sequential formulation of the blur operation. In this paper, we propose to use a variable blur model in the field by a variable linear combination of spatially invariant fuzzy functions.

In particular, we consider a constant PSF per zone with regular transitions between the zones to avoid edge effects. We also introduce a deconvolution method that is adapted to such modeling. More precisely, we use a fast method of deconvolution proposed in [11] which is based on an image decomposition strategy in order to perform parallel processing on sub-domains and thus accelerate computation time. We extend this method to the case of a spatially variable PSF according to the proposed model. We obtain an algorithm capable of reversing a variable PSF spatially by deconvolution in parallel on sub-areas of the image considered. The conditions at the edges of the zones are fixed in order to obtain a convergent algorithm towards the image sought. This avoids the approximations sometimes made during the deconvolution with a spatially variable PSF [7].

This work is organized according to the following steps: firstly, we present the PSF model that we used. Next, we describe the deconvolution method that we applied in this PSF model. Finally, we show the simulation results of the proposed approach on a synthetic image.

## 2. Non-stationary PSF model

The definition of a precise PSF model leads sometimes to consider a variant blur function at any point of the image. However, restoration with such a model remains a difficult problem. Indeed, when the impulse response of the imaging system depends on the coordinates of the point of the object, we cannot express the direct problem of forming the image as a convolution between the object and the PSF. To reduce the numerical difficulty of the problem and keep algorithms fast, we propose to approach a spatially variable PSF by piecewise constant PSF model with regular transitions between the zones. We decompose the discrete support of an image

$$\Omega = \{x_1^1, \dots, x_{n_1}^1\} \times \{x_1^2, \dots, x_{n_1}^2\} \subset \mathbb{R}^2 \quad (1)$$

in  $D$  blocks following a decomposition strategy similar to that proposed in [11]. For simplification of writing, we present the method for a decomposition into two zones ( $D = 2$ ). We thus consider two sub-areas  $\Omega_k$ ,  $k = 1, 2$  such that adjacent sub-areas overlap:  $\Omega = \Omega_1 \cup \Omega_2$  and  $\Omega_1 \cap \Omega_2 \neq \emptyset$ .

Then, we associate to each zone a spatially invariant PSF  $h_k$ ,  $k = 1, 2$ . Moreover, the change of the PSF from one zone to another is not abrupt. The transitions between the zones are managed by weighting functions which make it possible to smooth the

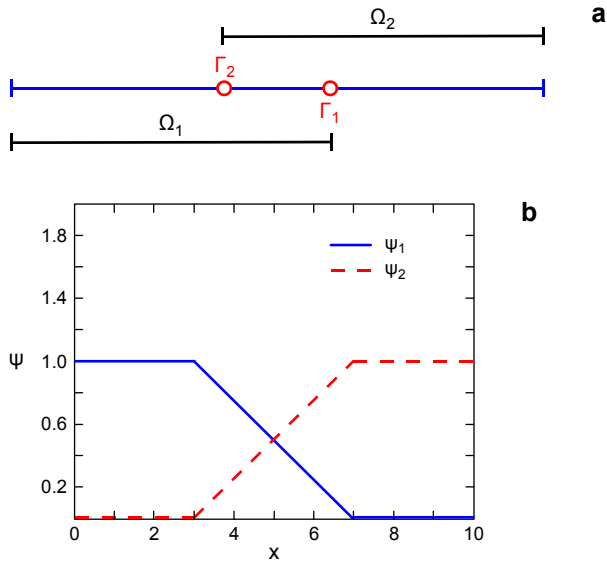


Fig. 1. Decomposition into two overlapping sub-domains (a), and example of weight functions  $\{\psi_1, \psi_2\}$  (b).

variations of the PSF between the zones. We introduce the functions  $\psi_1, \psi_2 \in \mathcal{H} = \{f: \Omega \rightarrow \mathbb{R}\}$  such that

- i)  $\psi_1(x) + \psi_2(x) = 1, \forall x \in \Omega$ , and
- ii)  $0 \leq \psi_k \leq 1$ , for  $k = 1, 2$ .

These functions act in the zone of intersection of the sub-areas. Their main role is to adjust the conduction of each of the fuzzy functions  $h_k, k = 1, 2$ , so as to smooth the variations of the PSF between the two zones. Thus, we define the object observation model through the following equation:

$$f(x) = \psi_1(x) \cdot (h_1 * u)(x) + \psi_2(x) \cdot (h_2 * u)(x) + b(x) \quad (2)$$

with  $u \in \mathcal{H}$  being the intensity of the original image,  $f \in \mathcal{H}$  the intensity of the degraded image and  $b(x)$  Gaussian white noise. By developing the equation of the model we can show that the convolution of the image  $u$  is performed by a spatially variable fuzzy function [12]. We thus introduce the operator  $R$  which indicates a “no stationary convolution”. An example of two-zone decomposition and an example of weight functions  $\{\psi_1, \psi_2\}$  are shown in Fig. 1.

### 3. Deconvolution of a blurred image by a non-stationary PSF

We will present a restoration method for spatially-variant blurred images. We considered a block constant PSF model. In this modeling, blocking artifacts are managed thanks to an overlapping domain decomposition strategy as well as the introduction of appropriate transition functions. Furthermore, object estimation within a framework of the considered space-varying PSF was achieved by minimizing a quadratic functional in-

cluding total variation regularization. For that matter, we extended an optimization method based on an overlapping domain decomposition technique to the case of space-varying PSF. Computational time is thus reduced by performing a parallel processing on different areas of the image at the same time. The convergence of the proposed method when using a space-varying PSF model was also proved thanks to certain constraints on the considered transition functions. In fact, the proposed algorithm works for any convex combination of stationary convolution operators and thus avoids the fastidious computation in the spatial domain when filtering with a space-varying filter [13]. Indeed, in the proposed blur modeling, stationary convolution can be rapidly computed in the Fourier domain and then combined together using a space-varying weighting function. Besides, we should emphasize that the accuracy of the restored image is highly dependent on the choice of a convenient domain decomposition considered in the observation model. In fact, each sub-domain should be approximated with the PSF. Automatic domain decomposition can be obtained by tolerating certain variation rate of the PSF within a given region, as it was previously proposed in [7]. In that method, a correlation coefficient between a reference PSF and each of the PSF measured at different points, was computed in order to measure the PSF variation rate and then used to define PSF positions.

Once we defined the imaging model, we seek to deconvolve the blurred image. To do this, we consider the problem of minimizing an energy function composed of two energy terms: the first is a quadratic term that corresponds to the fidelity to the data, and the second is a regularization term of type total variation which makes it possible to smooth the homogeneous zones of the image while preserving the contours. Consider the following energy function:

$$J(u) = \|\check{H}(u) - f\|_2^2 + 2\alpha \|\nabla u\|_1 \quad (3)$$

where  $\alpha > 0$  is a regularization parameter.

Although the operator  $\check{H}$  is spatially variable, it is possible to deconvolute with such an operator thanks to the modeling presented in the preceding paragraph. Indeed, the numerical calculation of the convolution by the non-stationary operator  $\check{H}$  is not carried out at any point separately, but it is carried out by calculating the sum of the stationary convolution products weighted by spatially variable weight functions. Moreover, in order to have a fast algorithm, we propose to minimize the function  $J(u)$  with an optimization method which was recently developed in [11]. This method has been studied in the case of a spatially invariant operator. Its theoretical convergence has been proved under certain conditions [11]. It has been successfully applied to signal interpolation and image in painting problems. We propose to extend this method to the deconvolution problem with a spatially variable PSF according to the proposed model. The general idea of the method [11] is to subdivide the global minimization problem into sub-problems of reduced size in order to treat them in a parallel way. The domain  $\Omega$  is divided into  $N$  sub-rectangular areas covering. For example, we consider a similar decompo-

sition to that presented in the previous section for the definition of PSF model. Note that it is possible to use decomposition in zones of more irregular shapes as long as they satisfy a property of division of the total variation explicated in [11].

The advantage of covering between zones is to avoid a fine analysis in the proof of convergence of the method at the level of the interface  $\Gamma_1$  between  $\Omega_1$  and  $\Omega_2 \setminus \Omega_1$  and the interface  $\Gamma_2$  between  $\Omega_2$  and  $\Omega_1 \setminus \Omega_2$ . We introduce the sub-spaces  $V_k$  of  $H$  such that  $V_k = \{u \in H, \text{support}(u) \subset \Omega_k\}$ ,  $k = 1, 2$ . Thus, a possible representation of the solution  $u \in H$  is given as follows:

$$u(x) = \begin{cases} u_1(x) & \text{if } x \in \Omega_1 \setminus \Omega_2 \\ u_1(x) + u_2(x) & \text{if } x \in \Omega_1 \cap \Omega_2 \\ u_2(x) & \text{if } x \in \Omega_2 \setminus \Omega_1 \end{cases} \quad (4)$$

where  $u_1(x) \in V_1$  and  $u_2(x) \in V_2$ . By using this decomposition, the minimization of the function  $J(\cdot)$  can be performed on each of the sub-areas separately. Let us for example minimize the functional with respect to  $u_1$  in the domain

$$\Omega_1: u_1 = \underset{u_1 \in V_1 / u_1|_{\Gamma_1} = 0}{\text{Arg Min}} J(u_1 + u_2) \quad (5)$$

FORNASIER *et al.* propose to perform this local minimization with a Lagrange multiplier method [11] which consists in minimizing an auxiliary function  $J_1^s(u_1 + u_2, u_1^{(l)})$  and  $J(u_1 + u_2)$  where  $u_1^{(l)} \in V_1$  in which the variable  $u_1$  is not affected by the operator  $\check{H}$ . This function is given by the following equation:

$$J_1^s(u_1 + u_2, u_1^{(l)}) = \|u_1 - z_1\|_2^2 + 2\alpha \|\nabla(u_1 + u_2)|_{\Omega_1}\|_1 \quad (6)$$

where

$$z_1 = u_1^{(l)} + \left\{ \check{H}^* \left[ f - \check{H}(u_2) - \check{H}(u_1^{(l)}) \right] \right\} \Big|_{\Omega_1} \quad (7)$$

and  $\check{H}(u_2)$  denotes the deputy of the non-stationary convolution operator  $H$ . As shown in [12] this operator is expressed in the following form:

$$\check{H}^*(v) = H_1^*(\psi_1 v) + H_2^*(\psi_2 v), \quad \forall v \in \mathcal{H} \quad (8)$$

where  $H_1^*(\cdot)$  and  $H_2^*(\cdot)$ ,  $H_1$  and  $h_2$  are respectively the deputy operators  $H_1(\cdot) = h_1^*$  and  $H_2(\cdot) = h_2^*$ . Thus, the minimizer of the function  $J_1^s(u_1 + u_2, u_1^{(l)})$  on  $u_1 \in V_1$  such that  $u_1|_{\Gamma_1} = 0$  is accessible thanks to an algorithm described in [11], based on an oblique thresholding theorem [11, 12]. We apply this principle to the restoration with the operator  $\check{H}$ . The convergence properties of the minimization method proposed in [11] are retained for the non-stationary operator. The theoretical study of conver-

gence is developed in [12]. We limit ourselves here to giving an algorithmic description of the proposed solution. The minimization algorithm consists in iterating on several processors the local minimizations in order to obtain partial solutions defined on each of the sub-areas considered. These solutions are then combined together via Eq. (4) in order to obtain an overall minimizer of the function (3). Thus, after initializing  $\check{u}_1^{(0)}$  and  $\check{u}_2^{(0)}$  such as  $u^{(0)} = \check{u}_1^{(0)} + \check{u}_2^{(0)}$ , global [11] consists in iterating the following four steps for decomposition into two sub-domains.

Step 1: energy minimization on the sub-domain  $\Omega_1$ . Initialize  $u_1^{(n+1, 0)} = \check{u}_1^{(n)}$ . For  $l$  from 0 to  $(L - 1)$ , iterate the following equation:

$$u_1^{(n+1, l+1)} = \underset{u_1 \in V_1/u_1|_{\Gamma_1=0}}{\text{Arg Min}} J_1^s(u_1 + \check{u}_1^{(n)}, u_1^{(n+1, l)})$$

Step 2: energy minimization on the sub-domain  $\Omega_2$ . Initialize  $u_2^{(n+1, 0)} = \check{u}_2^{(n)}$ . For  $m$  from 0 to  $(M - 1)$ , iterate the following equation:

$$u_2^{(n+1, m+1)} = \underset{u_2 \in V_2/u_2|_{\Gamma_2=0}}{\text{Arg Min}} J_2^s(u_2 + \check{u}_2^{(n)}, u_2^{(n+1, m)})$$

$$\text{Step 3: } u^{(n+1)} = \frac{u_1^{(n+1, L)} + u_2^{(n+1, M)} + u^{(n)}}{2}$$

$$\text{Step 4: } \begin{cases} \check{u}_1^{(n+1)} = \psi_1 u_1^{(n+1)} \\ \check{u}_2^{(n+1)} = \psi_2 u_2^{(n+1)} \end{cases}$$

The advantage of the minimization procedure presented is that it makes it possible to avoid the sequential and iterative formulation of the usual minimization methods which makes the calculation time quite slow. Indeed, steps 1 and 2 are performed in parallel on two processors. We show in the next paragraph that numerical experiments show good convergence properties in practice.

## 4. Simulation and result

We performed a first test on a synthetic image of size  $128 \times 128$  pixels, shown in Fig. 2a. We blurred this image with four different Gaussian PSFs, each corresponding to a given region. We thus consider overlapping domain decomposition into four sub-domains. Their interfaces are depicted in Fig. 2e. The red line corresponds to the lower side of the first rectangular sub-domain  $\Omega_1$ , the two green lines correspond to the interfaces of the sub-domain  $\Omega_2$ . The blue ones correspond to those of the third sub-domain  $\Omega_3$  and the yellow line represents the upper side of the sub-domain  $\Omega_4$ . Weighting functions as those displayed in Fig. 1 are considered in the proposed distortion modeling. We have thus considered functions of weights which vary according to the second dimension

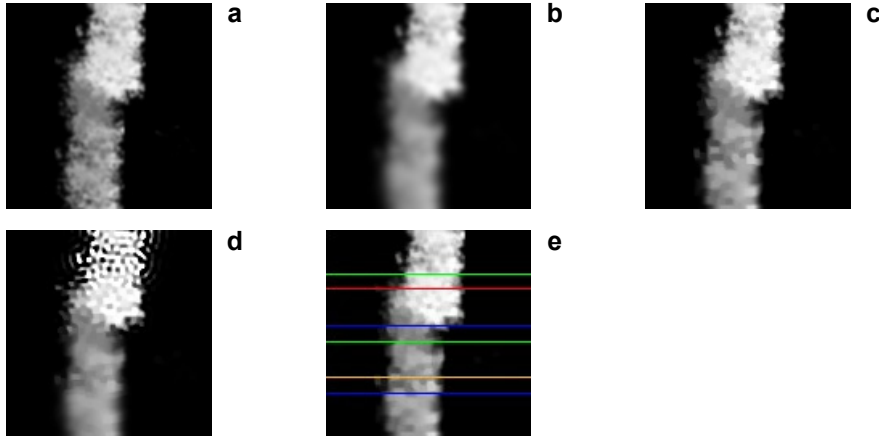


Fig. 2. Original image synthesis (a), blurred image with four Gaussian PSF (b), restored image (c), deconvolution with a spatially invariant PSF standard deviation  $\sigma = 2.125$  (d), and interfaces of the decomposition considered (four sub-domains) (e).

of the image (see Fig. 1b). Considering a blur variable in both directions of the image (such as the blur associated with astrophysical images), the weighting functions of the proposed model vary in both dimensions ( $x, y$ ) in order to manage the blur on the edges. We can, for example, choose variable weighting functions in  $x$  such as those shown in Fig. 1b when it is a horizontal transition between adjoining and variable domains in  $y$ , a vertical transition between domains. The sum of the values of the weighting functions must be 1 at any point of the image. In this test, we considered decomposition in 4 zones whose interfaces are shown in Fig. 2e. The PSFs considered are Gaussian with zero mean and standard deviations  $\sigma_1 = 1$ ,  $\sigma_2 = 1.75$ ,  $\sigma_3 = 2.5$  and  $\sigma_4 = 3.25$ . The resulting distorted images are depicted in Fig. 2b. The restored image displayed in Fig. 2c shows the relevance of the proposed deblurring method. Note that the reconstruction method was performed by considering the same decomposition as that used for the generation of the blurred image. The regularization parameter was fixed at  $\alpha = 2 \times 10^{-5}$ . The setting of this parameter was carried out in an empirical way, *i.e.*, we chose the parameter value which contributes to the best result. The algorithm converges after 20 iterations which lasted about 12 s for a decomposition into 4 sub-domains and 8 s for a decomposition into 8 sub-domains. We performed the tests on a multicore machine containing 4 processors of frequency 1.5 GHz. The method has been programmed with Matlab. The evolution curve of the energy function during the iterations (see Fig. 3a) shows the numerical convergence of the energy. In order to evaluate the method, we show in Fig. 3b the evolution curve of the mean square error (MSE) between the estimated image and the original image during the iterations. In order to see the contribution of the proposed restoration method, we present in Fig. 2 the deconvolution result with an invariant PSF having a zero mean and a standard deviation equal to the mean of the four

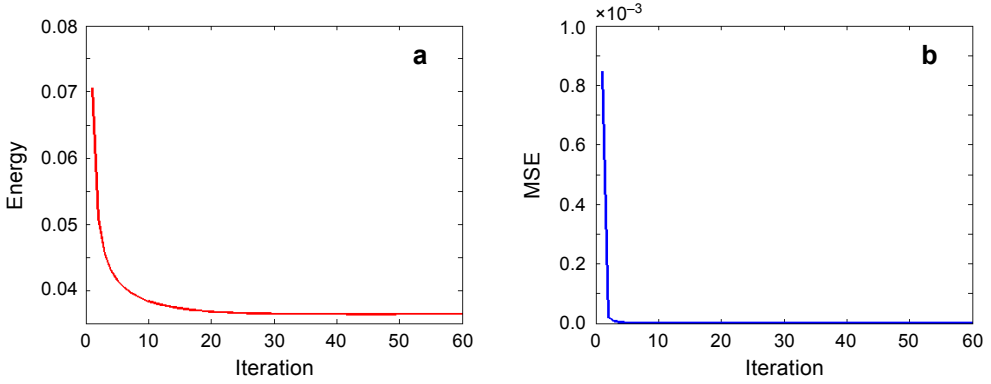


Fig. 3. Evolution of the energy function (a), evolution of the MSE as a function of the iterations (b).

standard deviations of the four PSFs used for the image degradation ( $\sigma = 2.125$ ). One can notice restoration especially in the higher and lower regions of the restored image of Fig. 2d. We calculated the MSE between the estimated object  $u(x)$  and the original one  $o(x)$  using the following formula to assess the accuracy of our estimation method:

$$\text{MSE}(u, o) = \frac{1}{\text{card}(\Omega)} \sum_{x \in \Omega} [u(x) - o(x)]^2 \quad (9)$$

In order to clearly see the advantage of the proposed restoration method, we show in Fig. 4 the plots of the intensity profiles along the optical axis passing through the bead center. The red curve corresponds to the intensity profile of the original object, the green curve corresponds to the observation intensity profile, the blue curve corresponds to the restored object with the space non-invariance approach and the dashed black

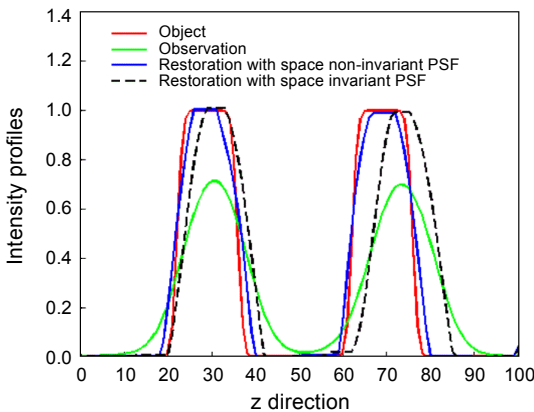


Fig. 4. The plot of intensity profiles along the optical axis passing through the center of the microspheres. The red line corresponds to the original object, the green line corresponds to the blurred object, the blue line corresponds to the restored object with the space-variant restoration approach and the dashed black line corresponds to the restored object with space-varying PSF.



curve shows the intensity profile of a restored object with the space-invariance assumption.

Numerical experiments show the efficiency of the proposed restoration method and the potential interest of the space-varying PSF model. Besides, we should emphasize that the accuracy of the restored image is highly dependent on the choice of a convenient domain decomposition considered in the observation model. In fact, in each sub-domain where the blur-variation could be considered as insignificant, we consider a single approximate PSF. Automatic domain decomposition can be obtained by tolerating certain variation rate of the PSF within a given region, as it was previously proposed in [9]. In that method, a correlation coefficient between a reference PSF and each of the PSF measured at different points, was computed in order to measure the PSF variation rate and then used to define PSF positions.

We were interested in minimizing a criterion including a data term computed as a quadratic error between the actual acquisition and the observation according to the model. This data term corresponds perfectly to an additive Gaussian noise context. However, if we deal with a multiplicative noisy image, *e.g.*, Poisson noise, the energy function cannot be written in a surrogate function form. Hence, it should be interesting to fit the proposed restoration method to the multiplicative noise case. Moreover, in the presented deconvolution method, we considered only one regularizing term which corresponds to total variation. It could be interesting to incorporate other regularizing terms such as wavelet regularization mainly to avoid the staircase artifact introduced by total variation. In that case, one should study the splitting of the regularizing criterion as it was previously done in [11].

## 5. Conclusion

We have presented in this paper a fast method of non-stationary deconvolution where a constant zone-specific PSF model has been considered. After having defined the spatially variable PSF model, we adapted a deconvolution method based on a zone minimization strategy of an energy function. The computation time is thus accelerated by performing parallel processing on the various areas of the image. The simulation of the method on a synthetic image shows its effectiveness.

Its application to real images, in particular images of fluorescence microscopy or astrophysical images, is possible by equipping itself with a map of PSF measured in the different regions where the blur can be considered invariant. Moreover, in several situations, the fuzziness associated with the acquisition system varies in a way that is not predictable *a priori* as a function of the acquisition conditions and of the scene observed.

It is then interesting to estimate the spatially variable vagueness and to extend the proposed method to the case of blind deconvolution. Moreover, in the proposed deconvolution method, we used a regularization term by total variation. It is possible to improve the restoration results by introducing a more appropriate regularization term such as regularization on the wavelet coefficients [14] in order to avoid certain artifacts

introduced by the total variation (the staircase effect). In this case, it will be necessary to propose the transformations necessary to apply the minimization algorithm by decomposition into sub-domains.

## References

- [1] PAWLEY J.B., *Fundamental limits in confocal microscopy*, [In] *Handbook of Biological Confocal Microscopy*, 1972, pp. 636–641.
- [2] HYO-KYUNG SUNG, HEUNG-MOON CHOI, *Nonlinear restoration of spatially varying blurred images using self-organizing neural network*, Proceedings of the 1998 IEEE International Conference on Acoustics, Speech and Signal Processing, Vol. 2, Seattle, WA, USA, 1998, pp. 1097–1100.
- [3] MEZOUARI S., HARVEY A.R., *Phase pupil functions for reduction of defocus and spherical aberrations*, Optics Letters **28**(10), 2003, pp. 771–773.
- [4] PANKAJAKSHAN P., BO ZHANG, BLANC-FÉRAUD L., KAM Z., OLIVO-MARIN J.-C., ZERUBIA J., *Blind deconvolution for thin-layered confocal imaging*, Applied Optics **48**(22), 2009, pp. 4437–4448.
- [5] PREZA C., CONCHELLO J.-A., *Depth-variant maximum-likelihood restoration for three-dimensional fluorescence microscopy*, Journal of the Optical Society of America A **21**(9), 2004, pp. 1593–1601.
- [6] MAGIERA A., *Point spread function in a confocal microscope with trigonometric pupil filters*, Optica Applicata **30**(2–3), 2000, pp. 455–461.
- [7] MAALOUF E., *Contribution to fluorescence microscopy, 3D thick samples deconvolution and depth-variant PSF*, PhD Thesis, Université de Haute Alsace – Mulhous, 2010.
- [8] NAGY J.G., O’LEARY D.P., *Restoring images degraded by spatially variant blur*, SIAM Journal on Scientific Computing **19**(4), 1998, pp. 1063–1082.
- [9] HIRSCH M., SRA S., SCHÖLKOPF B., HARMELING S., *Efficient filter flow for space-variant multiframe blind deconvolution*, 2010 IEEE Computer Society Conference on Computer Vision and Pattern Recognition, 2010 pp. 607–614.
- [10] BRIERS J.D., *Laser speckle contrast imaging for measuring blood flow*, Optica Applicata **37**(1–2), 2007, pp. 139–152.
- [11] FORNASIER M., LANGER A., SCHÖNLIEB C.-B., *A convergent overlapping domain decomposition method for total variation minimization*, Numerische Mathematik **116**(4), 2010, pp. 645–685.
- [12] MIRAUT D., PORTILLA J., *Efficient shift-variant image restoration using deformable filtering (Part I)*, EURASIP Journal on Advances in Signal Processing, Vol. 2012, 2012, article ID 100.
- [13] CILIEGI P., LA CAMERA A., SCHREIBER L., BELLAZZINI M., BERTERO M., BOCCACCI P., DIOLAITI E., FOPPIANI I., LOMBINI M., MASSARI D., MONTEGRIFFO P., TALIA M., *Image restoration with spatially variable PSF*, Proceedings of SPIE **9148**, 2014, article ID 91482O.
- [14] CARLAVAN M., WEISS P., BLANC-FÉRAUD L., ZERUBIA J., *Algorithme rapide pour la restauration d’image régularisée sur les coefficients d’ondelettes*, GRETSI, 2009.

*Received December 16, 2016  
in revised form April 3, 2017*